Polarimetric Calibration Results and Error Budget for SAR-580 System

RK Hawkins[†], R Touzi[†], A Wind[†], K Murnaghan[‡], and CE Livingstone[♥]

[†]Canada Centre for Remote Sensing, 588 Booth St, Ottawa, K1A 0Y7, Canada;
Email: robert.hawkins@ccrs.nrcan.gc.ca, ridha.touzi@ccrs.nrcan.gc.ca, andrew.wind@ccrs.nrcan.gc.ca;

[‡]Isoceles Information Solutions, on contract to CCRS, Email: kevin.murnaghan@ccrs.nrcan.gc.ca;

[♥]Defense Research Establishment, Ottawa, 3701 Carling Ave, Ottawa, K1A 0K2, Canada;
Email: Chuck.Livingstone@dreo.dnd.ca

ABSTRACT

Polarimetric SAR capability was first demonstrated in the CCRS (Canada Centre for Remote Sensing) airborne SAR facility as an experimental X-band channel. Although this demonstration system had poor channel isolation, techniques were developed to show that under these conditions, it was possible to produce fully calibrated polarimetric data. That system was eventually abandoned in favour of a technically much improved C-band polarimeter. In November, 1996, the facility was transferred to Environment Canada who own and operate the facility. This paper reviews the technical implementation of the C-band polarimeter, the processing and calibration chain, and results from an extended period of stable operations. Calibration for this system involves use of external PARCs and trihedral corner reflectors deployed across the imaging swath. The paper also gives an error budget for the phase and amplitude calibration of the instrument.

INTRODUCTION

The CCRS airborne SAR system [1,2] was transferred to Environment Canada in 1996 and is owned and operated by the Emergency Science Division there. CCRS and DND (Department of National Defense) continue to use and evaluate the facility and explore its use in a number of applications [3,4]. The system can collect SAR data in a number of modes including along-track and cross-track interferometry. This paper addresses only the polarimetric SAR mode at C-band.

The system can be configured in two slant range resolutions with flexible geometry. It was designed with range compression in hardware using analogue SAW/SAW^{-1} devices followed by 6-bit ADCs. (This restricts the system's capability for point target measurements because of dynamic range limitations [5].) To cover the dynamic range across the swath due to the combination of range, antenna pattern, and target backscatter, the system employs a sensitivity timing control (STC) that applies a range-dependent gain to the received signal train modelled to balance the expected falloff. Because STC also introduces accompanying phase rotations, this function is normally not used during polarimetric data collections.

Similarly, the SAR system has real-time motion compensation which performs three functions: dynamic antenna steering in azimuth and elevation to compensate for roll, pitch, and drift of the aircraft; PRF diversity to maintain the same ground sampling regardless of the ground speed; and phase rotation of the digitized signal to compensate for deviations from desired track. Due to inertial navigation system accuracy limitations, the phase rotation is normally not activated during polarimetric acquisitions in favour of post flight motion compensation.

To limit the calibration variables, we have recently adopted a 'standard' geometry that has good radiometric balance over a limited swath and is applicable to land targets using this mode. This is illustrated in Fig. 1.

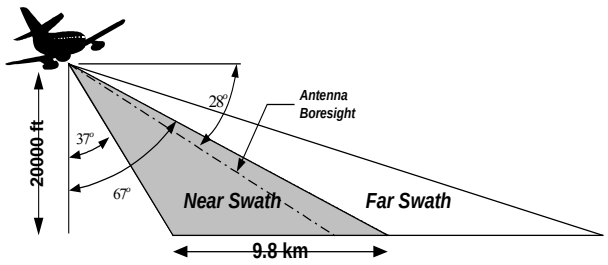

Fig. 1: Geometry for land applications with SAR

AMPLITUDE CALIBRATION

The amplitude calibration follows the method based on internal and external calibration using trihedral corner reflectors and PARCs (Polarimetric Active Radar Calibrators) instituted at CCRS [6, 7] to establish the absolute calibration at a few discrete points within the swath. The calibration is then extended across the swath using the antenna pattern determined on an antenna range [8]. Extension to other data sets that do not have external calibration devices is achieved by reference to an internal calibration signal generated using the BITE facilities of the radar, and measurements of the inherent noise floor of the instrument. Figure 2 shows a typical data acquisition sequence. In the figure, $DN_{tr}^{\ 2}$, DN'^2, and DN'^2_n are respective powers

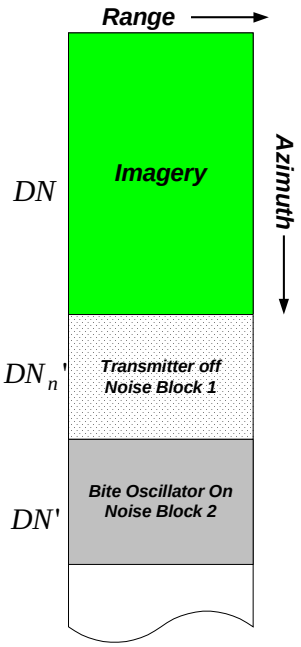

Fig. 2: Typical data acquisition sequence

of the processed scene and noise references before calibration. The basic radiometric calibration equation [7] used in the processing to radar brightness, β^o_{tr}, where *tr* indicates the transmit, receive polarization, is given by:

$$\beta^o_{tr} = \frac{DN_{tr}^2 - DN_n^2}{\left\langle DN'^2 \right\rangle} \times \frac{v}{P_{av}} \times \frac{R^3}{G_{tr}(\vartheta)} \times \frac{g_{sys}'}{g_{sys}} \times \frac{1}{K'_{tr}} \qquad \textbf{(1)}$$

Here, $\frac{v}{P_{av}}$ is the ratio of the ground speed to average radiated power; R is the range to the pixel; G_{tr} is the two-way antenna gain; ϑ is the antenna departure angle from boresight; $\frac{g'_{sys}}{g_{sys}}$ is the ratio of the system gain settings during the BITE acquisition to imagery acquisition; and K'_{tr} is the calibration constant dependent on polarization derived from point target measurements. Table 1 shows the results of a series of recent calibration measurements. The calibration constants here are the weighted mean of the individual targets, where the fading estimate is used as the weighting.

Table 1: List of amplitude calibration constants

Date	K'_{HH}	K'_{HV}	K'_{VV}	K'_{VH}
19-Jun-98	117.00	129.94	119.51	131.66
09-Jul-98	117.17	130.89	119.59	130.59
29-Jul-98	117.33	131.43	120.00	131.13
22-Oct-98	115.83	130.56	118.49	130.90
09-Mar-99	117.05	131.79	119.87	130.97
09-Mar-99	116.11	132.01	118.92	131.33
13-Apr-99	116.49	129.79	118.63	129.90
μ	**116.71**	**130.92**	**119.29**	**130.93**
σ	**0.57**	**0.87**	**0.60**	**0.57**
σ_μ	**0.22**	**0.33**	**0.23**	**0.21**

PHASE CALIBRATION

Polarimetry was first tested at X-band in 1991 using a polarimetric switch with poor channel isolation. Investigation of the amplitude and phase calibration of this system led to a general formulation of the polarimetric calibration problem [9]. The methodology involves use of several trihedral reflectors and repeating, time delay PARCs in the image to be calibrated.

With the C-band polarimeter, the isolation between the channels is high as can be seen from Table 2, so that calibration of the later C-band polarimetric instrument could proceed with a much simpler method in which the channels could be considered independently with essentially no mixing [10].

The corner reflectors (CRs) provide results for the amplitude and phase of the like polarizations and the PARCs, deployed in a $45^o \times 45^o$ orientation as shown in Fig. 4. This provides equal backscatter in all polarizations, and by comparison, allows determination of the cross-polarizations. Phase corrections relative to HH polarization determined in this way are then applied as a phase rotation to the complex data from the processor [11]. Table 3 shows recent results from this procedure.

Table 2: C-band polarimetric channel isolations

Property	$\frac{E_{HH}^2}{E_{HV}^2}$ (dB)	$\frac{E_{VV}^2}{E_{VH}^2}$ (dB)
Switch [12]	>50	>50
Antenna [13]	>37	>37
Total [14]	>35	>35

In these tables, μ represents the weighted mean; σ, the standard deviation; and, σ_μ, the standard deviation of the mean. These variations show that the calibration constants vary slightly from day to day, but are reasonably consistent. These difference may, however, be significant for some applications. Results from the cross polarization show more variation which may reflect the fact that fewer reflectors make up the mean for each day. In the case of parallel polarizations, approximately 20 reflectors may be used.

Fig. 3: PARC as deployed in a field situation

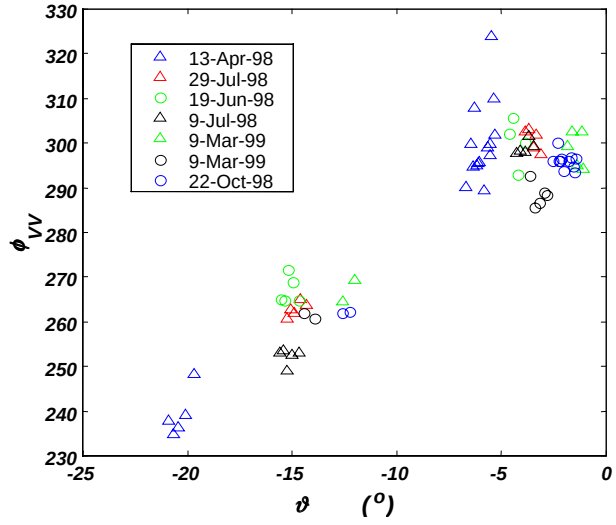

Fig. 4: Measured across track ϕ_{VV} phase variation

Table 3: Relative phase calibration constants

Date	ϕ_{HV} (deg)	ϕ_{VV} (deg)	ϕ_{VH} (deg)
19-Jun-98	102.63	287.65	85.78
09-Jul-98	90.04	286.87	82.38
29-Jul-98	94.60	296.43	87.23
22-Oct-98	110.95	297.69	98.13
09-Mar-99	106.91	288.32	84.35
09-Mar-99	97.32	302.10	89.02
13-Apr-99	103.53	290.45	93.15
μ	**100.85**	**292.79**	**88.58**
σ	**7.28**	**5.93**	**5.45**
σ_μ	**2.75**	**2.24**	**2.06**

The assessment of relative phase calibration across the swath has received less attention with this system since it was expected to be constant. Fig. 5 shows antenna angle dependence of the ϕ_{VV} phase rotation. This variation shown near the peak of the pattern is modest, but away from the mainlobe, substantial correction is required. We do not know the cause of this effect but it appears to be antenna gain related, and cannot be due to phase centre displacements as the effect is too large. Figure 5 shows a simple model of the effect of phase centre displacements observed in other radars15. The trend measured above would require a 16 cm displacement. Clearly more systematic investigation is required.

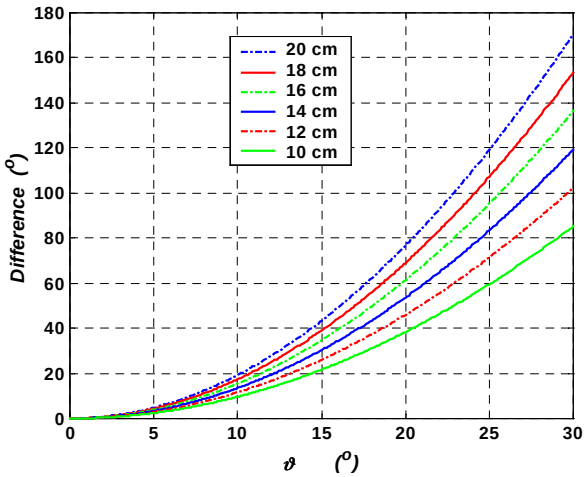

Fig. 5: Effect of phase centre displacement on ϕ_{VV}

ERROR BUDGET

The error budget for the system can be assessed in a number of ways including, through the statistics of the individual calibration measurements. The methods employed at CCRS normally involve use of two calibration arrays in the Ottawa area for local flights, and a PARC/CR combination in at least one flight line of remote acquisitions. This means that, at best, the overall calibration depends on the uncertainty in the associated calibration pass, our ability to extract and evaluate a set of $\{K'_{PP}\}$ data, and the accuracy with which we can extrapolate this temporally (between passes) and spatially (across and along swath). This may depend on differences in configuration of the system and the flying conditions (altitude, aircraft attitude etc.).

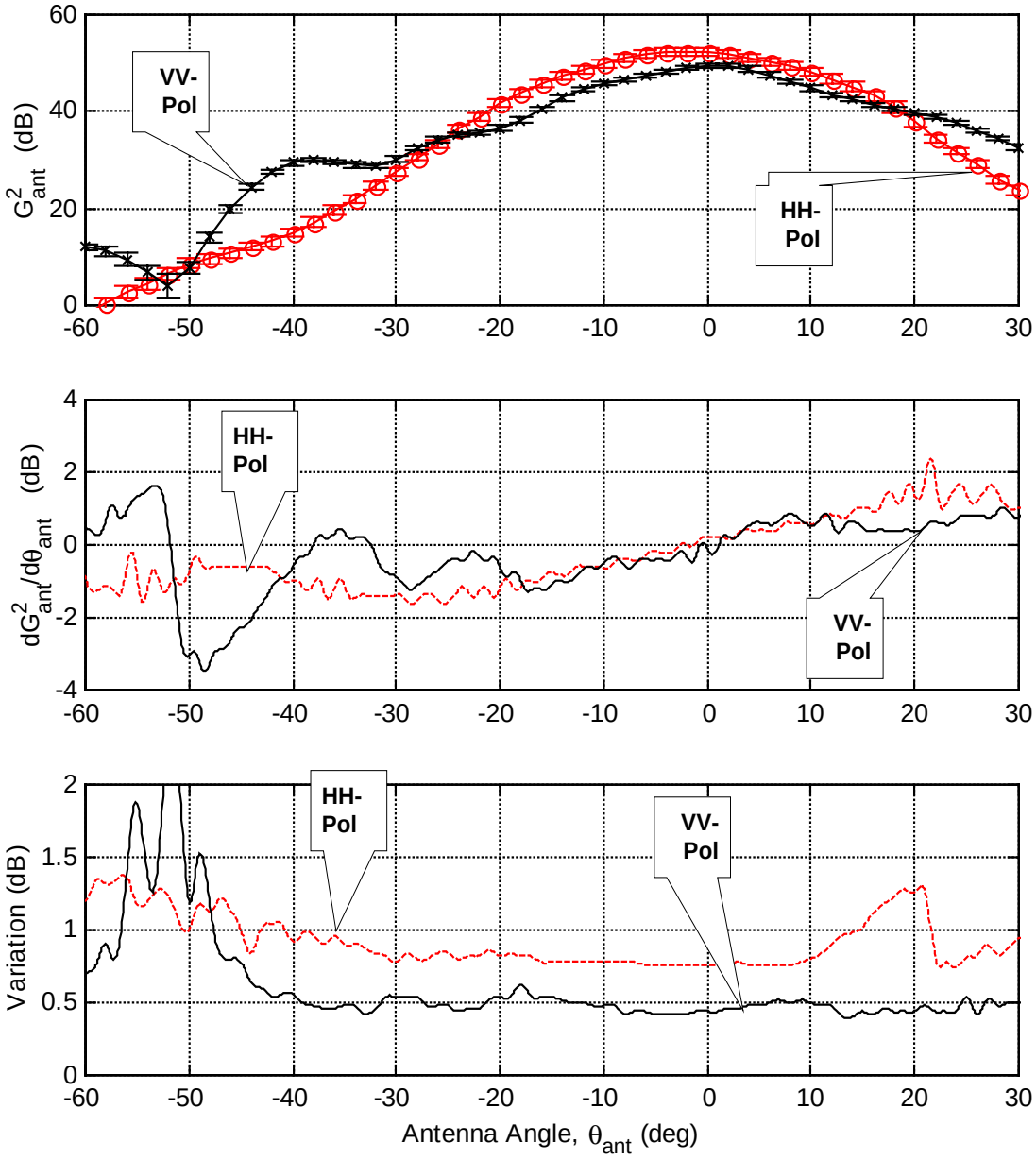

Fig. 6: Measured antenna gains for C-band SAR system. The error bars in the upper pane are shown as the variations at the bottom pane. The middle is the uncertainty in applied gain caused by a mask displacement of 1^o.

RADIOMETRIC ERROR BUDGET

Returning to (1) the two main contributing independent quantities come from the determination of the calibration constant K' itself and from $G_{tr}^2(\vartheta)$, the two-way antenna pattern. The other terms have small relative contributions.

$$\left(\frac{\Delta\beta^o}{\beta^o}\right)^2 = \left(\frac{\Delta K'}{K'}\right)^2 + \left(\frac{\Delta G_{tr}^2(\vartheta)}{G_{tr}^2(\vartheta)}\right)^2 + \ldots \quad \textbf{(2)}$$

The determination of K' requires an inversion of the radar equation form of (1) for point targets and involves knowledge of all the associated terms including the application of $G_{tr}^2(\vartheta_T)$ at the target, T, and its radar cross section. Let us assume that this uncertainty including background fading, and extraction error can all be determined from the relative spread in the measurements of the calibration constant, $\frac{\Delta K'}{K'}$.

Uncertainty in the antenna pattern, $\frac{\Delta G_{tr}^2(\vartheta)}{G_{tr}^2(\vartheta)}$ comes in two forms: the shape and size of the pattern; and the placement of the antenna mask over the illuminated swath. The antenna horn assembly is mounted in a radome beneath the aircraft near the tail on a three axis gimbal. The radiation path through the radome and the near field interaction of the antenna with the mounting faring and superstructure all depend on the aircraft attitude (pitch, roll, and yaw). As explained in [3], antenna range measurements were taken in the radome environment at various attitude configurations to assess these influences on G_{tr}^2; these are plotted in Fig. 6. Within ±20° of the boresight, these are approximately constant in level at 0.7 dB for HH polarization and 0.5 dB for VV polarization.

We note that the dynamic range represented in an airborne image is especially high (50-60 dB) compared to typical spaceborne systems which cover much smaller angular ranges within their swaths. Placing this mask correctly over the resultant imagery requires accurate knowledge of the antenna pointing. Considerable effort [16] has been placed in matching the observed behaviour of CRs and distributed targets in the swath to determine the actual position of the antenna pattern relative to the readout and control information from the system. From this study, we believe that the mask can be placed within ±0.3°. Returning to Fig. 5, this kind of uncertainty would lead to radiometric uncertainty which varies with angle to a maximum of 0.3 dB within ±20° of the boresight.

Combining these ideas, we provide in Table 4 our estimates for the overall RMS errors expected from this system based on the calibration information derived from the data and presented above. Results from a particular line might be improved by site specific calibration. The results are over a region of ±20° of the boresight of the antenna.

Table 4: Systematic error budget

Property	**Unit**	**Within a Pass**	**Between Passes**
$\frac{d}{d\vartheta}G_{tr}^2(\vartheta)\Delta\vartheta$	(dB)	0.70	0.70
ΔG_{tr}^2	(dB)	0.30	0.30
$\Delta K'$	(dB)	0.30	0.70
Total	(dB)	**0.80**	**0.99**
$\Delta\phi$ within ±10° of peak	(deg)	3	10
$\Delta\phi$ beyond ±10° of peak	(deg)	30	30

CONCLUSIONS

This paper has reviewed some recent polarimetric calibration results from the CV-580 C-band SAR. It shows the difficulty and importance of polarimetric calibration, even for a very well isolated system. This suggests that the engineering effort and procedures required for satellite systems need to be considered carefully.

ACKNOWLEDGEMENTS

We thank the pilots and crew of the DOE CV-580 aircraft : Bryan Healey, Bill Chevrier, Reid Whetter, Doug Percy for their skills and efforts in making data acquisitions possible; Rob Gould, Rob Nelson and Paul Daleman for maintenance and support of this complex system. Ideas for processing and calibration with resultant operational code have been developed over an extended time by many individuals including: Paris Vachon, John Campbell, Laurence Gray, Tom Lukowski, Paul Daleman, John Wolfe, Mike Adair, Lana Ikkers (Teany), Ping Leung, Simon Methot, Gerrit Wessels, Peter Farris-Manning, Karim Mattar, Wendy Liu, Ian Neesan and Stephan Nedelcu to name only a few. Ronny Jean and Simon Austin assisted in

processing the data. It is a pleasure to acknowledge their contributions and accomplishments.

REFERENCES

1 Livingstone *et al*., "The CCRS airborne SAR systems: Radar for remote sensing research," *Can. J. Rem. Sens*,. vol. 21, No. 4, 1995, pp. 468-491.

2 Minister of Supply and Services, Canada Centre for Remote Sensing Airborne C/X SAR, Cat. No M77-42/1994E, ISBN 0-662-22886-3,1994.

3 Hawkins *et al*., "Calibration and use of CV-580 airborne polarimetric SAR data," *Proc. 4th International Airborne Remote Sensing Conference and Exhibition/ 21st Canadian Symp. Rem. Sensing*, vol. 2, 1999, pp.32-40.

4 R Touzi, "On the use of polarimetric SAR data for ship detection," *IGARSS'99 Proceedings*, 1999, 4p.

5 RK Hawkins and PW Vachon , "C/X SAR Gain and Point Target Measurements – The Saturation Problem," CCRS internal documentation, CCRS-TN-1998-26, 1998, 10p.

6 LMH Ulander *et al.,* "Absolute Radiometric Calibration of the CCRS SAR," *IEEE Transactions on Geoscience and Remote Sensing*, November 1991, p. 922-933.

7 RK Hawkins and P Daleman, "Calibration Implementation for the CCRS Airborne SAR", DMD-TM-90-724, 1991, 100p.

8 SYK Tam *et al.,* "Calibration of the CCRS airborne SAR antenna –Final Report," SSC File No. 018SR.23413-8-4158, 1989, 151p.

9 R Touzi CE Livingstone, JRC Lafontaine, and TI Lukowski, "Consideration of antenna gain and phase patterns for calibration of polarimetric SAR data,", *IEEE GSRS*, vol. 31, No. 6, 1993, pp. 1132-1145.

10 R Touzi and S Nedelcu, "Calibration of the polarimetric Convair-580 C-band SAR. Technical Report," CCRS/DREO agreement FY 97/98-98/99, Nov. 98, 20p.

11 A Wind, "Polarimetric calibration of the CCRS SAR data June 19 to July 29th, 1998," CCRS-TN-1999-010, 1999, 32p.

12 Acceptance testing done by *COMDEV* verified by DREO.

13 Notes from acceptance testing at *COMDEV*.

14 CE Livingstone, personal communication regarding 1993 field trials.

15 RJ Decker and A van den Broek, "Calibration of polarimetric Pharus data," CEOS SAR Workshop, ESA publication WPP-138, 1998, pp. 353-357.

16 RK Hawkins *et al*., "C/X SAR, POLGASP, antenna pattern, and antenna pointing," CCRS internal technical note, CCRS-TN-1999-12, 1999, 12p.